Shell disintegration and taphonomic loss in rudist biostromes

DIETHARD SANDERS

LETHAIA

Sanders, D. 1999 07 15: Shell disintegration and taphonomic loss in rudist biostromes. *Lethaia*, Vol. 32, pp. 101–112. Oslo. ISSN 0024-1164.

Radiolitid biostromes in the Upper Cretaceous of Austria and Italy record a marked taphonomic loss controlled mainly by the composition of the biocoenosis, by the density of rudist colonization, by the style of radiolitid shell disintegration and by early diagenetic processes. Radiolitid shells consisted of a calcitic ostracum and an originally aragonitic hypostracum. The attached valve of most radiolitids was built of (1) an outermost ostracal layer of delicate calcite lamellae, (2) a thick layer of 'boxwork ostracum' built of radial funnel plates and cell walls, (3) a thin, inner 'ostracal layer 3' of thick-walled boxwork, and (4) the hypostracum that formed the innermost shell layer. The attached valve disintegrated by spalling of radial funnel plates of layer 2, and by selective removal of the boxwork ostracum. In the free valve, the ostracum consisted of two layers: (a) an inner, lid-shaped layer of dense calcite, and (b) an outer layer composed of calcite lamellae. The free valve disintegrated by spalling into ostracal and hypostracal portions, by spalling of the ostracum into layers a and b, and by disintegration of layer b into packages of calcite lamellae and individual lamellae. The specific style of disintegration of the radiolitids was aided or induced by discontinuities in shell structure. Lamellar fragments from the ostracum of the upper valve and from the radial funnel plates of the lower valve locally are abundant in free-valve – funnel-plate floatstones that comprise the matrix of or occur in lenses within radiolitid biostromes. In biostromes with an open parautochthonous fabric, selective removal of the boxwork ostracum of the attached valve occurred by mechanical spalling and, most probably, by early diagenetic dissolution. Complete removal of the boxwork ostracum yielded thin, relict shells composed of the 'ostracal layer 3' and the hypostracum. During early diagenesis, the hypostracum was replaced by blocky calcite spar, or was dissolved and became filled by internal sediments. The combination of both selective removal of boxwork ostracum and early diagenetic dissolution of aragonite locally resulted in the formation of ghost biostromes that entirely or largely consist of faint relics of radiolitids. The syndepositional formation of radiolitid shell relics and the presence of radiolitid ghost biostromes produced by biostratinomic and early diagenetic processes show that rudist biostromes can undergo marked taphonomic loss during fossilization. The presence of ghost biostromes with a burrowed, open parautochthonous rudist fabric indicates that the final preservation of a rudist biostrome was directly influenced by the characteristics of the biocoenosis, including unpreserved burrowing taxa. Rudist biostromes may be of markedly different taphonomy as a result of the taxonomic composition of the entire assemblage and the density of colonization by the rudists. □*Taphonomy, taphonomic loss, rudists, radiolitids, rudist biostromes.*

Diethard Sanders [diethard.g.sanders@uibk.ac.at], Institute for Geology and Paleontology, University of Innsbruck, Innrain 52, A-6020 Innsbruck, Austria; 9th April, 1998; revised 18th February, 1999.

Biostratinomic processes that influence a biotic assemblage during and shortly after its life are typically closely related in space and time to early diagenesis, and together they comprise the taphonomy of that assemblage. The resulting taphocoenosis may significantly depart from the living biotic community (e.g., Lawrence 1968; Fürsich & Aberhan 1990). Cretaceous rudist formations have long been studied with respect to paleontology, sedimentology and diagenesis (e.g., Toucas 1903, 1907; Zapfe 1937; Kühn 1967; Skelton 1976, 1978, Skelton *et al.* 1995; Bebout & Loucks 1977; Pons 1977, 1982; Enos 1988; Minero 1988; Koch *et al.* 1989; Ross & Skelton 1993; Alsharhan 1995; Sanders 1996a, 1998a; Sanders & Baron-Szabo 1997; Sanders *et al.* 1997; Sanders & Pons 1999). In previous literature, however, the taphonomy of rudist communities has received little attention. As rudist communities inhabited shallow neritic environments that are inherently unstable in their physical, chemical and biological conditions (e.g., Coe 1957; Stanton & Dodd 1976; Scott 1978; Fürsich & Aberhan 1990), a significant impact of taphonomic processes on the accumulation and preservation of rudist constructions may be expected.

In this paper, the styles and the possible processes of shell disintegration of Late Cretaceous radiolitid rudists

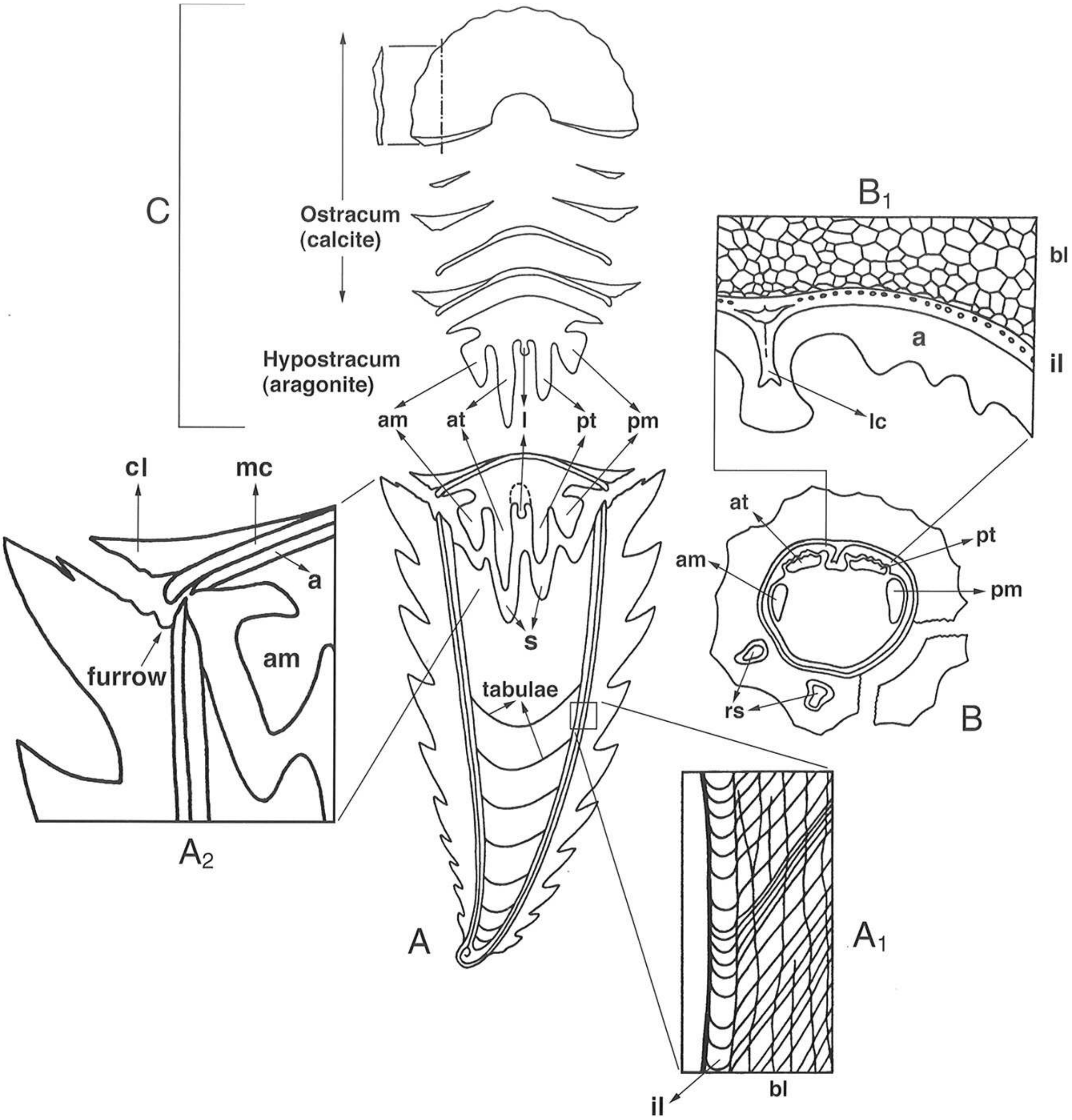

Fig. 1. Main features of radiolitid shell. □A. Axial section, showing the cone-shaped attached (lower) valve and the cap-like free (upper) valve. The attached valve was subdivided by tabulae composed of hypostracal aragonite. Along their margin, the tabulae merged into a hypostracal layer on the inner side of the shell; this layer also comprised the sockets (s) for the teeth of the upper valve. In the upper valve, the hypostracal, aragonitic shell part built the anterior myophore (am), anterior tooth (at), ligament (l), posterior tooth (pt), and posterior myophore (pm). □A_1. The ostracum of the attached valve consists of a thin, inner layer (il) composed of a relatively thick-walled boxwork structure and a thick outer layer of thin-walled boxwork (bl). □A_2. Detail of the commissural region. In the upper valve, the aragonitic hypostracum (a) is overlain by a layer of 'massive' calcite (mc) which, in turn, is overlain by a layer composed of stacked, delicate calcite lamellae (cl; see also Fig. 2F). The outer edge of the massive calcite layer (mc) fits into a furrow in the lower valve. □B. Transverse section, with formation of relic shell by spalling of the ostracal layer (bl; the boxwork ostracum) away from the inner ostracal layer (il in A_1) indicated. In transverse section, the radial structures (rs), the anterior myophore (am), the anterior tooth (at), and the posterior tooth (pt) and posterior myophore (pm) are visible. □B_1. Detail of transverse section near the ligamentary crest (lc), with the hypostracal, aragonitic shell layer (a) indicated. The inner boxwork layer of the ostracum (il) extends into the inner part of the ligamentary crest, and locally forms a small gap near the base of the crest. The inner layer of the ostracum may consist of more-or-less dense calcite with only a few, subcircular pores. The outer, thick, boxwork layer (bl) of the ostracum contains a thin layer of small irregular cells at its base. □C. Typical pattern of disintegration of the free valve into aragonitic (hypostracal) and calcitic (ostracal) parts. The calcitic portion of the free valve disintegrated either into packages of calcite lamellae that may be of circular shape or into smaller platy fragments.

are described. In particular, the selective removal of the boxwork ostracum of the shell and the role of a hitherto little appreciated ostracal layer, and its consequences for the preservation of radiolitid biostromes, are described. The rudist formations described in this paper were studied in a number of localities in the Upper Cretaceous (Gosau Group) of the Eastern Alps, Austria, and from the succession of the Karst platform in Northern Italy. The results of the study imply that entire radiolitid biostromes became nearly completely erased by the combined effects of biostratinomic and early diagenetic processes.

The radiolitid shell

The shell of radiolitids consisted of a hypostracum of aragonite and an ostracum of calcite (Fig. 1; e.g., Zapfe 1937; Kennedy & Taylor 1968; Amico 1978; Cestari & Sartorio 1995). In the lower, attached valve of most radiolitids, three outer layers of ostracum and an inner layer of hypostracum can be distinguished. The ostracal shell layers consisted originally of calcite, and thus are often well preserved. The aragonitic, hypostracal layers, however, generally are preserved as blocky calcite spar. The shell layers of the attached valve are:

1. The outer ostracal shell layer typically is less than a millimeter to about 3 mm in thickness (the latter in large specimens), and consists of delicate calcite lamellae, each much less than a millimeter thick (Fig. 2C); because of its thinness and external position, this layer is rarely preserved completely (see also Amico 1978).
2. The middle, thick ostracal layer (labelled 'bl' in detail A_1, Fig. 1) typically consists of a delicate boxwork built by horizontal radial funnel plates and vertical cell walls (e.g., Amico 1978). In each radial layer, the vertical cell walls develop from upward folds from the underlying radial funnel plate (Amico 1978; Pons & Vicens 1986). Locally, the vertical cell walls are not developed, giving rise to composite lamellae, each consisting of a 'stack' of radial funnel plates (Fig. 3A).
3. The inner layer of the ostracum (labelled 'il' in detail A_1, Fig. 1) ranges in thickness (depending on the size of the radiolitid specimen) from about 0.5 to 4 mm. It consists of a single array of relatively thick-walled boxwork structure in which the radial plates have a downward-convex shape. The vertical spacing of the radial plates closely resembles the vertical spacing of the radial funnel plates in the boxwork ostracum, but with a systematic vertical offset across a continuous wall of calcite (see A_1 in Figs. 1, 2A, B). In other specimens, the inner layer consists of a thick-walled boxwork with subcircular 'pores' in transverse section (Fig. 2C, D). The described inner ostracal layer extends into and builds the inner part of the ligamentary crest. In many specimens, at the base of the ligamentary crest there is a small gap between the two ostracal layers (detail B_1, Figs. 1, 2D). As is outlined below, the described 'ostracal shell layer 3' played a crucial role in the taphonomy of radiolitids.
4. The hypostracum was originally aragonitic and provided the tabulae, the attachment scars for the adductors, and the sockets for the teeth of the cardinal apparatus of the free valve (Fig. 1; see, e.g., Cestari & Sartorio 1995).

In the free valve, the inner, hypostracal part, including teeth, myophores and ligament, was built of aragonite, whereas in the outer part, the ostracum consists of calcite (Fig. 1; Cestari & Sartorio 1995). The ostracum consists of two distinct parts, (a) an inner, lid-shaped layer of calcite that, internally, appears poorly structured in the optical microscope, and (b) an outer layer composed of a stack of delicate calcite lamellae (Fig. 2E, F; see also Cestari & Sartorio 1995, p. 36). In the outer ostracal layer, both the entire stack of calcite lamellae as well as the individual laminae become thinner and pinch out towards the topmost point of the valve, but are curved and thicken towards the commissural surface with the lower valve (Figs. 1C, 2F).

Along the shell commissure, the 'lid-like' inner ostracal layer of the free valve protrudes slightly; the protrusion fits into a furrow of the lower valve (detail A_2 in Fig. 1). From the inner part of the lower valve, in turn, a slight protrusion extends into a small gap between the ostracal and the hypostracal portion of the free valve. The furrow along the commissural surface of the lower valve (see A_2 in Fig. 1) corresponds to the downward-convex shape of the radial plates in the 'ostracal shell layer 3' of the lower valve (see A_1 in Fig. 1; compare Fig. 2A, B). The ostracal shell layer 3 of the lower valve and the 'lid' of the inner ostracal layer (a) of the free valve thus correspond in their position (see A_2 in Fig. 1). Where the radial structures approach the commissure, the furrow may be widened and deepened (see e.g., Cestari & Sartorio 1995, p. 36).

Shell disintegration

Fragmentation of radiolitid shells that has not been controlled by shell structure or original mineralogy can be commonly observed, particularly in layers of radiolitid rudstone that formed by fragmentation of rudists during high-energy events (e.g., Sanders 1996a). Within radiolitid biostromes, however, disintegration controlled by shell structure and mineralogy was widespread, and affected both the lower, attached valve and the free, upper valve.

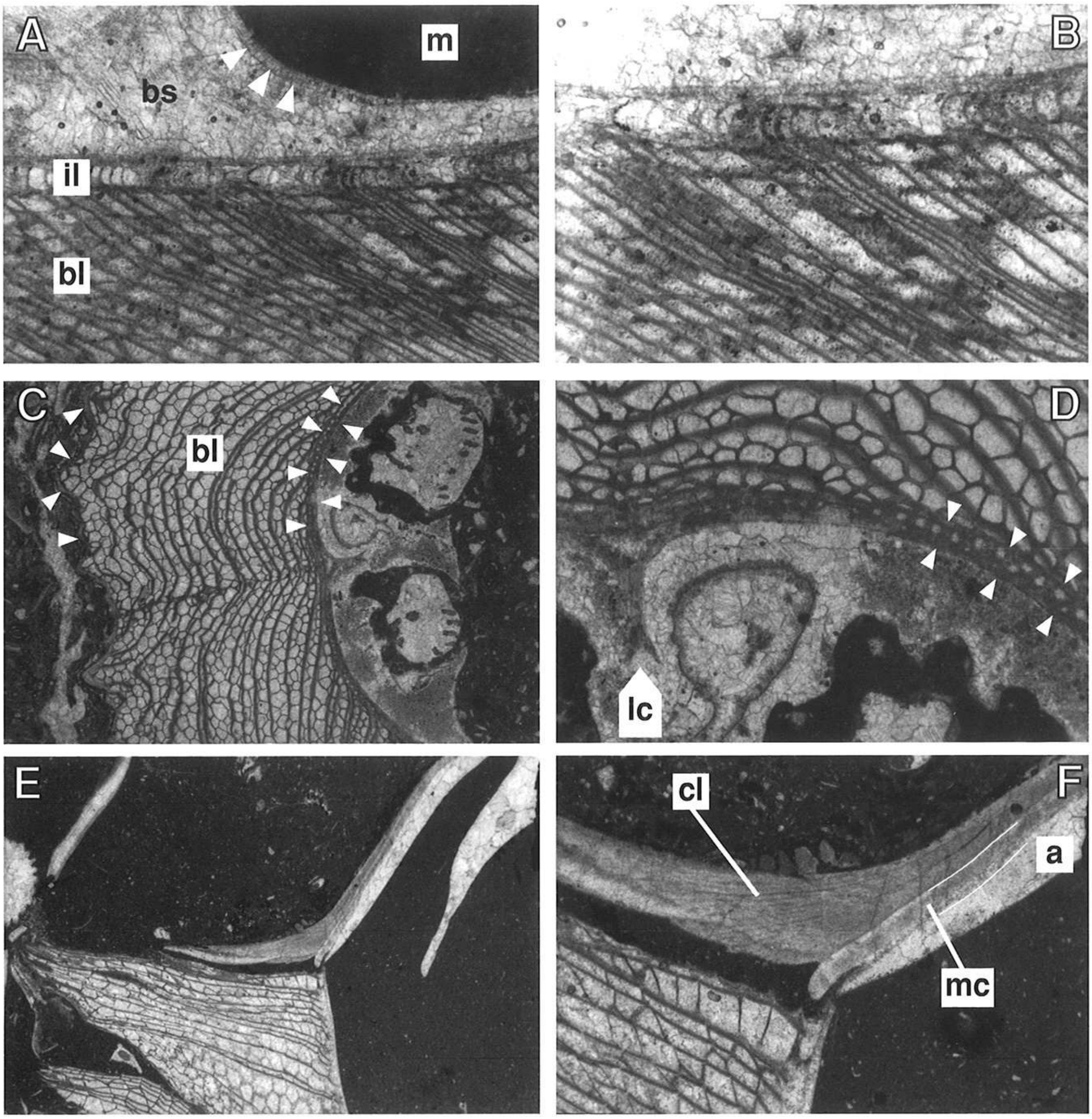

Fig. 2. Thin section views of the features illustrated in Fig. 1. □A. Detail of axial section through a radiolitid shell, showing body cavity of mussel filled by lime mudstone (m), separated from the underlying intertabular space (filled by blocky calcite spar; bs) by a tabula formerly composed of aragonite showing relic structure (arrowtips). Aside from the tabula, the hypostracal shell layer is hardly visible. The ostracum consists of an inner layer (il) with a densely spaced, thick-walled boxwork structure, and a thick outer layer (bl) composed of delicate boxwork. Width of view 5.3 mm. □B. Detail from A. Note the downward-convex shape of the radial plates in the inner ostracal layer, and that the spacing of the radial plates of the inner layer follows the same pattern as the radial funnel plates in the outer, thick boxwork layer. Width of view 3.5 mm. □C. Transverse section through a radiolitid lower valve, showing the cardinal teeth, the ligamentary crest, and the outer part of the shell. The hypostracal, formerly aragonitic parts of the cardinal apparatus have been replaced by calcite spar and, locally, by a light grey microsparite. The ostracum consists of a thin but relatively thick-walled inner layer (delimited by arrowtips) with subcircular cells, a thick middle layer (bl) composed of delicate boxwork cells, and an outermost layer (indicated by arrowtips) composed of a stack of very thin calcite lamellae. Width of view 17 mm. □D. Detail from C showing the thick-walled, inner ostracal layer (delimited by arrowtips) with subcircular cells, and the extension of the inner lamella of this layer into the ligamentary crest (lc). Width of view 5.3 mm. □E. Axial section through the commissural region of a radiolitid. The upper valve consists of an inner layer of former aragonite, now replaced by blocky calcite spar, and an outer layer of calcite. Width of view 17 mm. □F. Detail from E. The formerly aragonitic, hypostracal part (a) of the free valve has been replaced by blocky calcite spar. The calcitic part of the free valve consists of an inner layer of 'massive' calcite (mc; delimited by thin white lines) and an outer layer (cl) of stacked calcite lamellae. At the commissure, the layer of 'massive' calcite shows a small, 'eyelid-like' protrusion that fits with a radial furrow in the ostracum of the lower valve. Along the inner part of the lower valve, in turn, a slight protrusion extends into a small gap between the inner, calcitic and the aragonitic part of the free valve. The furrow at the commissural surface of the lower valve (cf. A_2 in Fig. 1) reflects the downward-convex shape of the radial funnel plates in the inner ostracal layer of the lower valve (cf. Fig. 2B). Width of view 5.5 mm.

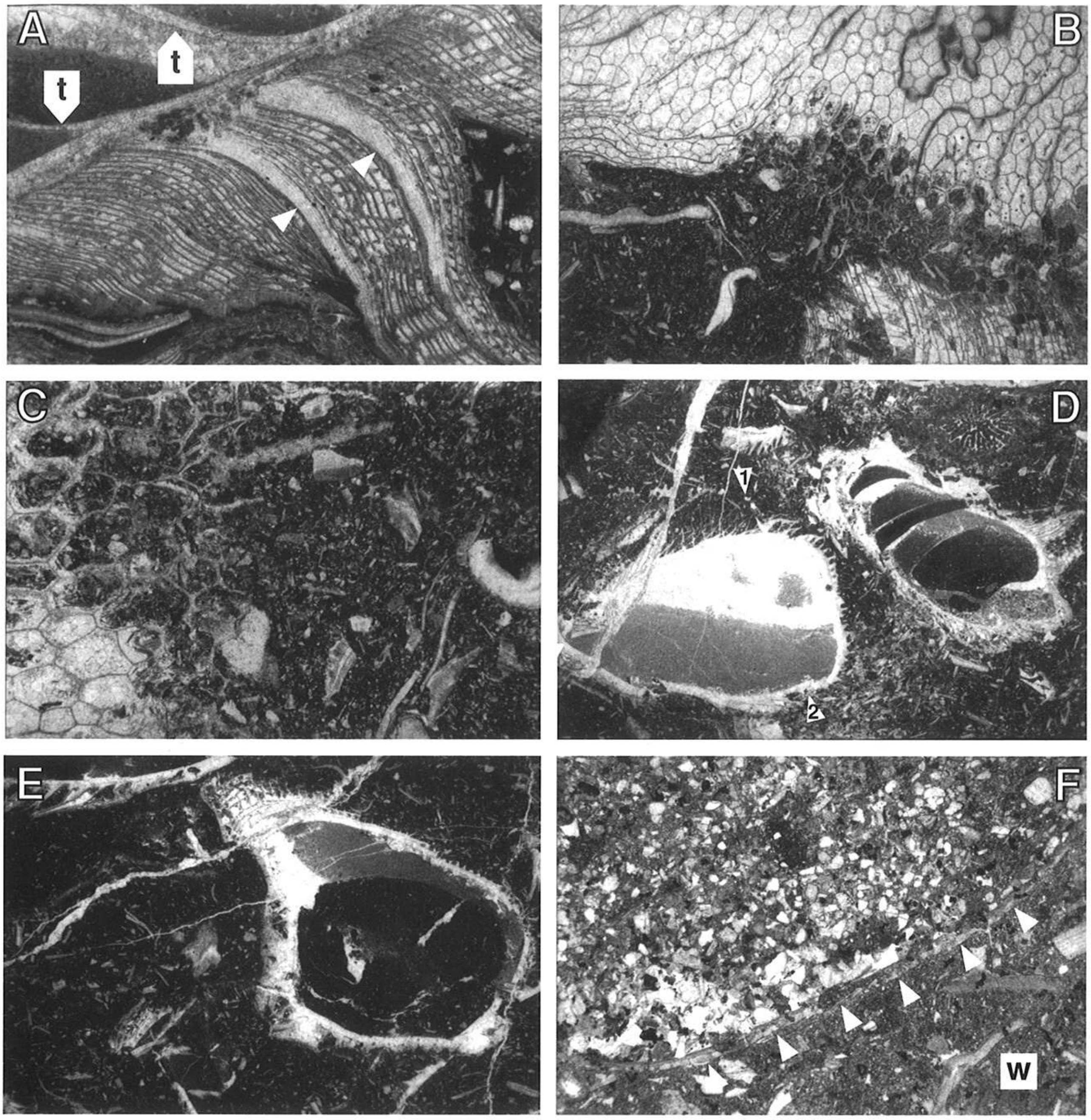

Fig. 3. □A. Detail of axial section through a radiolitid. The hypostracal (formerly aragonitic) shell parts are relatively well preserved and show the merging of the tabulae (t) into the hypostracal layer on the inner side of the shell. The intertabular spaces are geopetally filled by a micropeloidal grainstone to packstone. In the boxwork ostracum, the radial funnel plates locally are merged into layers (marked by white arrowtips) composed exclusively of radial funnel plates. Width of view 10 mm. □B. Detail from a biostrome with an open, parautochthonous fabric, showing the disintegration of the boxwork ostracum. Width of view 17 mm. □C. Detail from B. The boxwork ostracum disintegrates into abundant delicate fragments in the silt- to mud size-range. Locally, these fragments comprise the major part of the small-sized bioclasts in the matrix. Width of view 6.8 mm. □D. Detail from a radiolitid biostrome with an open, parautochthonous fabric. Note the bioturbation and the local, gradual thinning-out (arrowtip 1) of the boxwork ostracum. Where the boxwork ostracum has been completely removed, only the more robust, inner ostracal shell layer remained (arrowtip 2). The shells are geopetally filled mainly by micropeloidal packstone to grainstone. Width of view 17 mm. □E. Motif similar to D. The shell has been largely dismantled from its boxwork ostracum, save a few remnants. The matrix is a microbioclastic wackestone with abundant silt-sized bioclasts derived from fragmentation mainly of the boxwork ostracum. Width of view 17 mm. □F. Detail from a radiolitid biostrome. The matrix of the biostrome is a poorly sorted bioclastic wackestone (w) with a microbioclastic matrix. A thin, relic shell of a radiolitid composed of the inner ostracal shell layer (marked by arrowtips) is filled by a coarse bioclastic packstone. Width of view 17 mm.

Disintegration of the attached valve

For the lower valve of radiolitids, a selective removal of both the thin, outermost ostracal shell layer and of the comparatively thick layer of boxwork ostracum was common. Selective removal of the boxwork ostracum has been observed in radiolitid biostromes that consist of bioturbated floatstones with a high amount of disoriented radiolitids (open, parautochthonous rudist fabric; Sanders 1996b; Sanders & Pons 1999). The larger burrows in these floatstones are as much as several centimeters in diameter and locally contain spreiten structure. The matrix of these rudist floatstones typically is a rudist-clastic wackestone or, less commonly, a bioclastic packstone to fine sand bioclastic grainstone.

Commonly, an overall gradual disintegration and removal of the boxwork ostracum is indicated (Fig. 3B). The disintegration of the boxwork yielded fine sand to silt-sized bioclastic material that is a very common constituent in the matrix of biostromes with an open, parautochthonous fabric (Fig. 3C). Locally, the walls of the boxwork ostracum become progressively thinner down to zero from the inner, better-preserved part of the boxwork to its outer margin (Fig. 3D). Alternatively, the boxwork ostracum appears to have been removed by spalling. Where the process of gradual dismantling or spalling was stopped in an early stage, incompletely dismantled radiolitid shells are preserved (e.g., Figs. 3B, 5B; see also Cestari & Sartorio 1995, p. 41). Where disintegration and removal of boxwork was complete, only a relict shell remained, composed of the inner, thin ostracal shell layer 3, and the formerly aragonitic hypostracum. In thin section, the relict shells are recognizable by small remnants of ostracum (Fig. 3D, E). In other cases, however, the removal of the boxwork was quite complete (Fig. 3F).

Locally, large chunks of boxwork ostracum that comprise the entire thickness of the layer can be observed in the close vicinity of relict radiolitid shells (e.g., Fig. 4). These chunks evidently spalled off along or near the boundary between the thin, 'inner ostracal layer 3' (i.e. the layer that makes up the radiolitid relics) and the ostracum (see Fig. 1B). Spalling of boxwork ostracum is also suggested by radiolitid specimens that show a sharp, steep boundary between a relict shell part and a shell part with a thick layer of boxwork ostracum (e.g., Cestari & Sartorio 1995, p. 41). Even in well-preserved specimens, a very thin gap is often visible between the central part of the 'inner ostracal layer 3' and the outer shell layers (Figs. 2C, 6B). In their incipient stages, these gaps appear to originate from a lateral merging of the cells in the 'inner ostracal layer 3' (see Fig. 2C). When more evolved, the gaps typically show a slightly irregular thickness and irregular surface (Fig. 6B).

In the cases where the boxwork ostracum was entirely removed, biostromes composed more-or-less completely of 'rudist ghosts' result (Fig. 4). These *ghost biostromes* are hardly recognizable on naturally weathered outcrop surfaces. At first glance, the ghost fabrics resemble large burrows. The presence of diagnostic structures of radiolitids, including the inner calcitic shell layer (Fig. 3F), ligamentary crests (Figs. 4, 5A), the crescent-shaped, geopetal fills of the intertabular spaces (Sanders 1998a; see also Fig. 4), and the presence of partly dismantled radiolitids (Fig. 5B), however, reveal the correct nature of these structures. In densely packed radiolitid rudstones (packed, parautochthonous rudist fabric) and in radiolitid bafflestones (autochthonous rudist fabric; Sanders & Pons 1999), the described selective disintegration and removal of the boxwork ostracum was not observed; the feature thus seems to be specific to open radiolitid fabrics with bioturbation.

Disintegration of the free valve

Spalling of the calcitic part of the upper valve and of radial funnel plates of the lower valve is recorded by floatstones and, less commonly, rudstones that are largely composed of calcite lamellae from the free valve, of radial funnel plates, and of stacks of radial funnel plates (Figs. 1C, 6A). These *free-valve – funnel-plate floatstones* are a common lithology both within and in immediate vertical association with radiolitid biostromes, and typically occur in lenses a few centimeters to decimeters thick and a few centimeters to several meters in lateral extent (Sanders & Baron-Szabo 1997; Sanders 1998b; see also Amico 1978; Cestari & Sartorio 1995, p. 36). Where bedding planes of these floatstones are exposed, the surface may be scattered with the intact, disc-shaped calcitic part of the free valve (see Fig. 1C) and abundant large fragments thereof. In the free-valve – funnel-plate floatstones, fragments from the aragonitic parts of the free valve are subordinate to rare.

Aside from the mentioned shell fragments, these floatstones typically are devoid of other large bioclasts, notably of larger fragments from the boxwork ostracum of the lower valve. The matrix of these floatstones is a wackestone to mudstone with sand- to silt-sized rudist

Fig. 4. □A. Photograph from a radiolitid biostrome with an open, parautochthonous fabric, as exposed on a wetted surface cut by rope wire. The biostrome is largely composed of relic shells that consist only of the inner, ostracal layer of the lower valve (delicate white lines). The relic shells are filled by a slightly darker, coarse bioclastic packstone. □B. Line drawing of A. Black: large fragments from boxwork ostracum (R). H=*Hippurites nabresinensis*. Stippled patches show the infills of coarse bioclastic packstone into the relic shells, which are shown by thick lines; the shell relics are locally slightly crushed by compaction. Locally, within the packstone-filling, the former fillings of the intertabular spaces are present (if) and typically consist of laminated mudstone to bioclastic wackestone. A direct clue to the origin of the packstone fills from radiolitid rudists is given by the local presence of the inner layer of the ligamentary crest (arrows 1, 2).

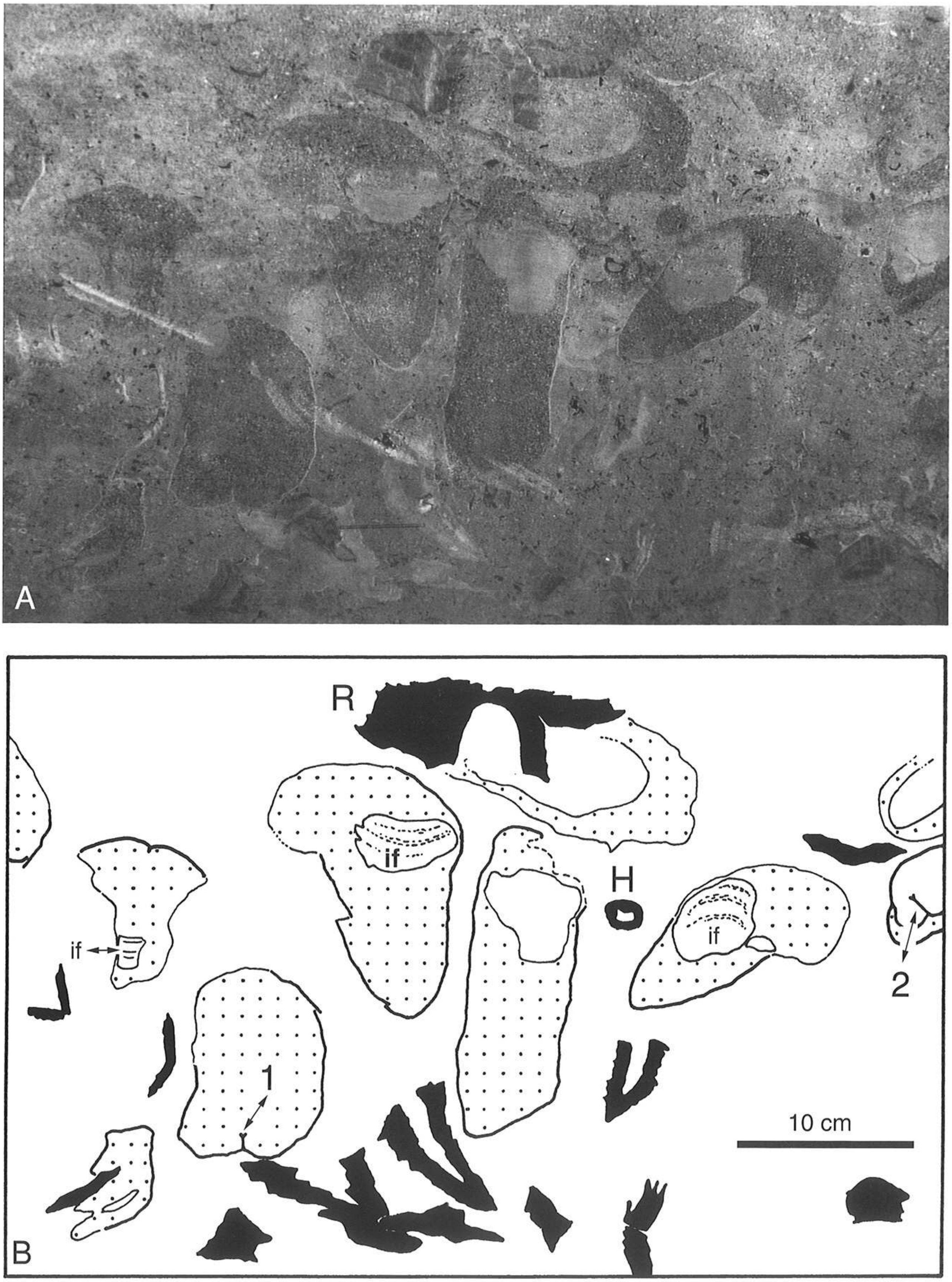
A
R
if
H
if
if
2
1
10 cm
B

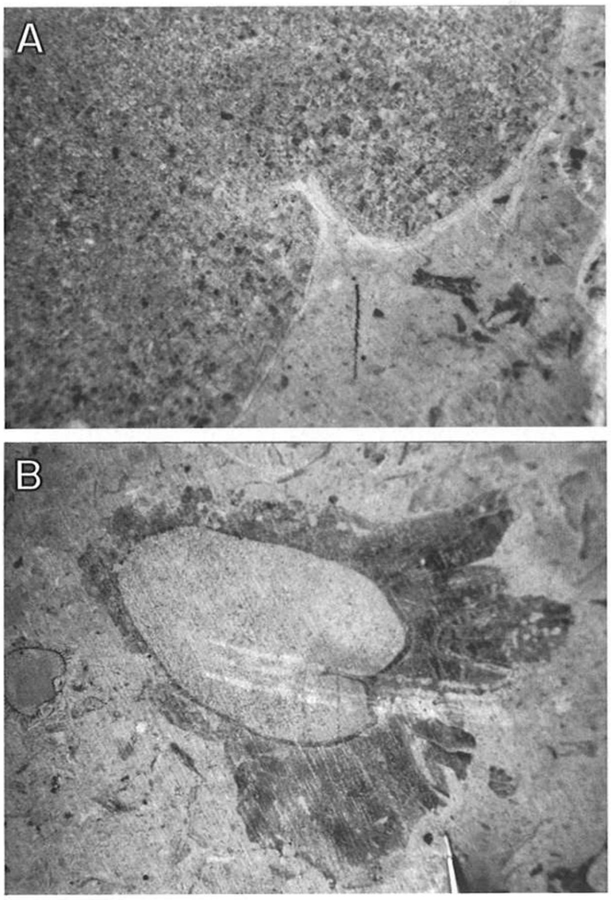

Fig. 5. □A. Detail from a relic ligamentary crest from a biostrome as shown in Fig. 4. Width of view 6.5 cm. □B. Radiolitid shell, only partly dismantled from the boxwork ostracum. Note the well-visible thin inner shell layer of the ostracum, and its direct extension into the ligamentary crest. Width of view about 8.5 cm.

fragments, smaller benthic foraminifera and fragments from calcareous green algae. Because of mechanical compaction of the lime-mud matrix, the described rudist fragments may be more-or-less crushed. Both the more-or-less complete ostracal and hypostracal parts of the free valve can often be found as isolated, well-preserved specimens.

Early diagenetic overprint

During early diagenesis, the aragonitic hypostracum of radiolitids was generally, and with equal likelihood, either replaced by blocky calcite spar or dissolved and filled by internal sediments, such as lime mudstone, micropeloidal wackestone to packstone to grainstone, or bioclastic wackestone to packstone to grainstone. In many cases, the internal sediment of limestone is identical or closely similar in both composition and texture to strata that closely overlie the biostrome along an emersion surface. Dissolution of aragonite in an early stage is also indicated by the compaction-induced deformation of the semi-lithified sedimentary fills of the intertabular spaces of the lower radiolitid valves (Sanders 1998a). The dissolution of the hypostracum was independent from the biostratinomy of the calcitic ostracum. Thus, radiolitids with a well-preserved ostracum may have their hypostracum dissolved and filled by blocky calcite spar or by internal sediment (Fig. 6B).

In many radiolitid biostromes with an open parautochthonous fabric, however, both the selective removal of the boxwork ostracum and early diagenetic dissolution of aragonite combined to result in ghost biostromes. These ghost biostromes entirely or largely consist of radiolitid relics each composed of the more-or-less deformed crescent-shaped sedimentary fills of the intertabular spaces, hosted by the thin 'ostracal shell layer 3' (cf. Sanders 1998a) (Fig. 6C, D). Such ghost biostromes are hardly recognizable on the surface of naturally weathered limestones, and also escape recognition by applying the standard field technique of examining small rock chips with the hand lens.

Interpretation and discussion

In previous literature, neither the distinct microstructure of the described inner ostracal layer of the lower valve nor its significance for the taphonomy of radiolitids has been appreciated. The inner ostracal layer, however, is clearly visible in many of the transverse sections photographed by Toucas (1907), Amico (1978) and Cestari & Sartorio (1995), and appears to be a common feature of many, if not all, genera of radiolitids. Although it is evident in many of the thin-section photographs of Amico (1978), it is only mentioned in the caption to Pl. 29 for several genera of sauvagesiine radiolitids: a 'rangée de cellules initiales (CI) sur le pourtour de la cavité générale'. The inner ostracal shell layer is not mentioned or described as a separate structural entity, however (Amico 1978). Few thin-section photographs of the inner ostracal layer have been published with both sufficient magnification and preservation to allow a precise judgment of its structure (Amico 1978; Cestari & Sartorio 1995). The few photographs available suggest that the inner ostracal shell layer might be of slightly different structure in different radiolitid genera. The relation of the structure to ontogeny and environmental factors, however, is unknown. The inner ostracal shell layer may have escaped attention because, being common in a similar form in many radiolitid genera, it appears to be of little taxonomic value. Yet, precisely because it is a common feature, the inner shell layer is significant in radiolitid taphonomy.

The common presence of distinct types of shell fragments, particularly the evidence for spalling of boxwork

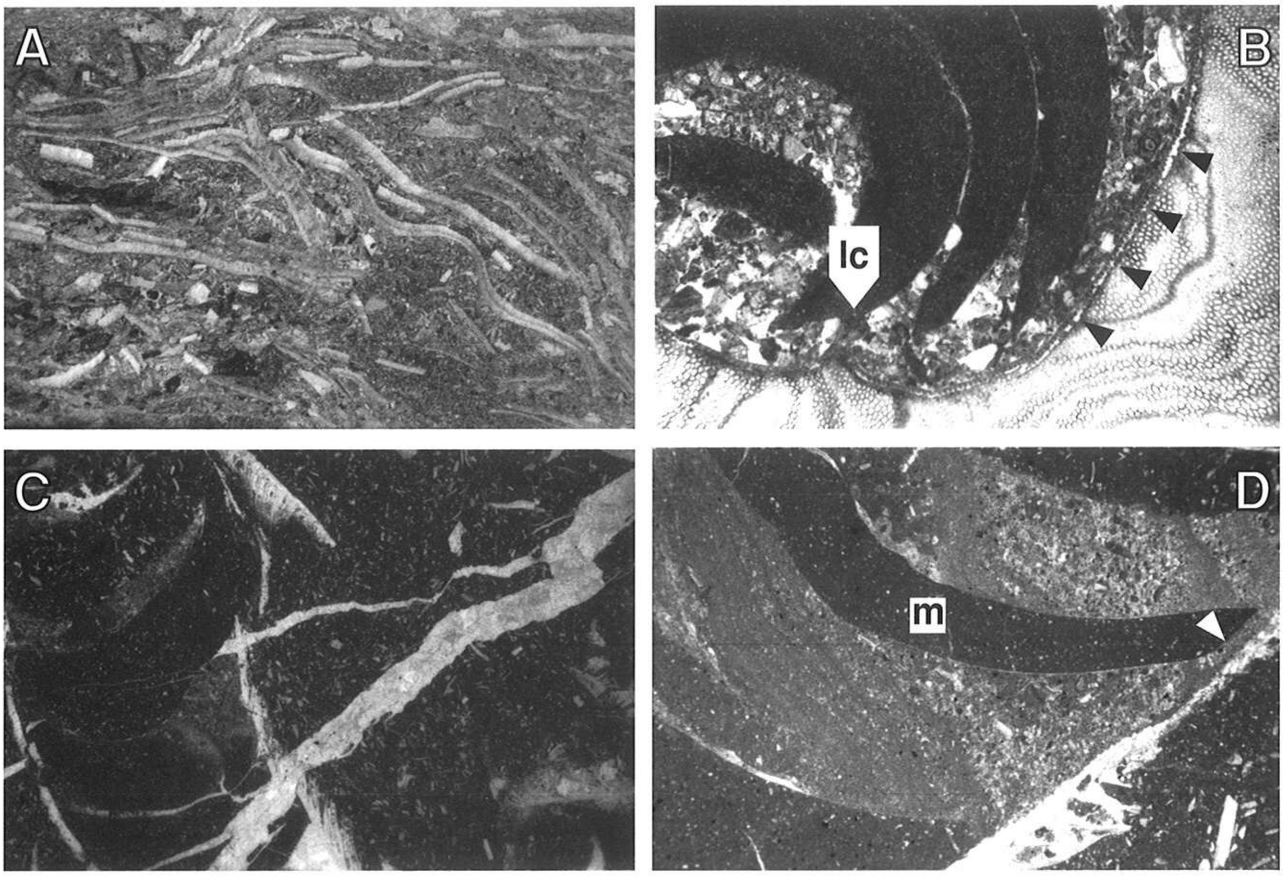

Fig. 6. □A. Floatstone to rudstone composed largely of platy fragments from radiolitid ostracum. Width of view 17 mm. □B. Oblique–transverse section through radiolitid with well-preserved ostracum that shows the thin, inner ostracal layer (arrowtips) and its extent into the ligamentary crest (lc). The aragonitic tabulae and the aragonitic inner shell layer have been dissolved and were later filled by bioclastic grainstone. Width of view 17 mm. □C. Detail from radiolitid biostrome with an open, parautochthonous fabric. In the left part of the photo, a 'radiolitid ghost' is recognizable only by the relic ostracal shell and the crescent-shaped fills of the intertabular spaces. The aragonite of the tabulae has been dissolved and became partly filled by a fine sand to silt bioclastic wackestone to mudstone. Width of view 17 mm. □D. 'Radiolitid ghost', showing a relic ostracal shell layer of the lower valve, and the crescent-shaped fills of the intertabular spaces. Note the difference in texture and sedimentary structures between the intertabular fills of a dark grey microbioclastic wackestone to mudstone (m), and light grey fills that consist of geopetally oriented, interlaminated microbioclastic packstone, wackestone and mudstone. On the inner side of the shell, the light grey fills are connected with each other along a 'channel' (arrowtip) that probably corresponds to the former hypostracal, aragonitic shell layer. Width of view 7.5 mm.

ostracum from the thin, inner ostracal layer, and the common presence of relict shells suggest a structural control over the disintegration of radiolitid shells. Disintegration may either have been controlled by discontinuities in the structure of different shell parts, and/or because of the presence of membranes of organic material between different parts of the shell. During and after decomposition of the organic membranes after death of the mussel, the shell may have disintegrated preferentially along the planes of structural weakness when subject to physical stress.

For the selective removal of the boxwork ostracum, both the influence of shell structure and biostratinomic processes probably were important. Selective removal has been observed only in parautochthonous radiolitid fabrics that show evidence for bioturbation; this strongly suggests that the texture of a radiolitid biostrome and the taphonomy of the radiolitids are genetically related. The described thinning of the walls of the boxwork cells probably results from dissolution of the shell while it was still in the soft, bioturbated sediment. Walter & Burton (1990) demonstrated that bioirrigation can lead to re-dissolution of significant amounts of carbonate, even in shallow subtidal sediments that are bathed by waters supersaturated (at least for most of the time) with respect to calcium carbonate. The effectiveness of calcium carbonate dissolution induced by bioirrigation may be enhanced by a rise in dissolved carbon dioxide during nocturnal cooling of the water (cf. Revelle & Emery 1957). In addition, decomposing organic material within the boxwork and invasion of the boxwork by bacteria may have produced microenvironments with a raised carbon dioxide level that may

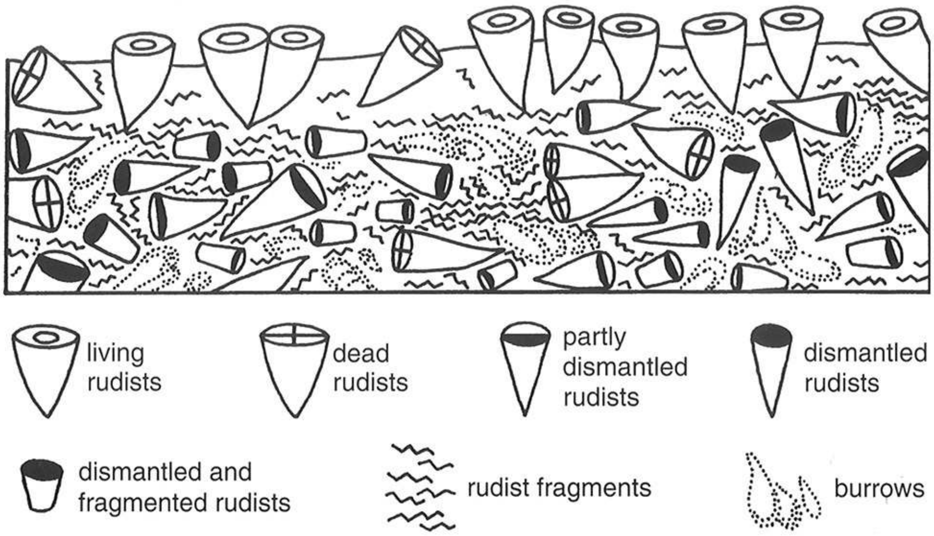

Fig. 7. Idealized scheme of a radiolitid biostrome with a bioturbated, open, parautochthonous fabric. These radiolitid biostromes are characterized by a mixture of complete, disoriented radiolitid shells ('dead rudists') with relict radiolitid shells that were more-or-less dismantled from their boxwork ostracum and coarsely fragmented before final burial. In addition, the aragonitic (hypostracal) shell parts of the radiolitids often have been replaced by blocky calcite spar and/or by internal sediment. Where the processes of dismantling of the ostracum and aragonite dissolution were widespread, ghost biostromes composed almost entirely of radiolitid shell relics were produced. See text for further description and discussion.

also have favoured dissolution. The combination of bioirrigation with the very large surface area of the boxwork ostracum and its delicate, compartmentalized construction favouring the establishment of diagenetic microenvironments thus may provide a partial explanation for its selective removal. The amount of dissolution-induced loss, however, is difficult to estimate. Churning of both the sediment and the rudists by burrowing organisms, and repeated episodes of burial–exhumation of the shells by bioturbation and by physical sedimentary processes, have led to progressive abrasion and spalling of the dissolution-weakened parts of the ostracum, and to dispersal of the delicate boxwork clasts into the matrix.

Spalling of chunks of the entire boxwork layer suggests that shell disintegration was influenced by shell structure. In many radiolitid specimens, because of its irregular shape, the described, thin gap between the central part of the 'inner ostracal layer 3' and the outer shell layers probably originated by dissolution. These gaps would have been a significant structural weakness within the shell. The presence of the gaps may give an explanation for the spalling of large parts of boxwork layers, provided that they are of very early diagenetic origin. Alternatively, the boundary between the 'inner ostracal shell layer 3' and the boxwork ostracum was a mechanically preferred site of spalling.

For the free valve, spalling of the hypostracal aragonitic from the ostracal calcitic shell part must have been common. More-or-less complete ostracal and hypostracal parts of the free valve are often found as isolated, well-preserved specimens in successions that have been deposited in paralic to basinal environments.

The specific composition of the free-valve – funnel-plate floatstones, including thin stacks of calcite lamellae as well as individual calcite lamellae, indicates that the calcitic shell parts readily disintegrated into their structural building blocks (cf. also Fig. 1C). Because of their thinness and platy shape, once put into transport the fragments from both the free valves and the radial funnel plates had a low hydraulic radius and could be moved by comparatively gentle currents. Free-valve – funnel-plate floatstones occur only in close association with radiolitid biostromes, indicating that these fragments were rapidly comminuted and diluted with other bioclastic material upon farther-distance transport. The wackestone to mudstone matrix, as well as the highly selective enrichment of the platy fragments, indicates that the deposition of these floatstones proceeded under medium to low water energy (see also Amico 1978, p. 112).

Significance for taphonomy

Free-valve – funnel-plate floatstone is a specific lithology that results from the shell structure and biostratinomy of radiolitids. The described phenomena and the possible processes of selective removal of boxwork ostracum, and their connection with radiolitid biostromes with an open, parautochthonous fabric provide an example of the control exerted on the preservation of a level-bottom community by the interrelation between substrate type, density of substrate colonization, physical environment, bioturbation and early diagenetic processes.

Rudist biostromes are thus not always preserved in an easily interpretable fashion but, as has been described for other level-bottom communities (cf. Stanton & Dodd 1976; Staff *et al.* 1986; Fürsich & Aberhan 1990), may undergo marked taphonomic change during fossilization (Fig. 7). The presence of relict radiolitid shells within burrowed, open, parautochthonous rudist fabrics indicates that the trophic structure of the living rudist community was not comparable to densely packed, paucispecific populations of epifaunal suspension feeders, but was of a mixed type with both epifaunal suspension feeders and infaunal detritus feeders. Such a trophic structure is typical for the less densely colonized margins of recent oyster banks, and for substrata scarcely colonized by oysters (cf. Scott 1978 and references therein). The presence of shell relics in ghost biostromes with an open, parautochthonous rudist fabric indicates that the final preservation of a rudist biostrome may have been directly influenced by the characteristics of the entire living community, including the unpreserved burrowing taxa (cf. Lawrence 1968), and the specific physical and chemical conditions produced in part by the community itself.

By contrast, rudist biostromes composed of very densely packed elevator rudists in upright position most probably had the trophic structure characteristic for dense populations of epifaunal suspension feeders, i.e. no or only a negligible proportion of burrowing organisms existed within the community. This implies that rudist biostromes may be of significantly different trophic structure and taphonomy, more or less as a direct result of the total population composition (preserved and unpreserved) and density of substrate colonization during the time when the biostrome accumulated (Sanders & Pons 1999).

Conclusions

The lower, attached valve of most radiolitids consisted of four shell layers: (1) an outermost, thin ostracal layer of delicate calcite lamellae, (2) a thick ostracal layer of a boxwork ('boxwork ostracum') built of radial funnel plates and cell walls, (3) a thin, inner ostracal layer that consists of a single layer of thick-walled boxwork (this 'ostracal layer 3' also built the inner part of the ligamentary crest), and (4) the aragonitic hypostracum that provided the innermost shell layer, the attachment scars for the adductors, the sockets for the teeth, and the tabulae. In the free valve the hypostracum included the teeth, myophores and the ligament. The ostracum consisted of two layers: (a) an inner, lid-shaped layer of calcite that appears poorly structured in the optical microscope, and (b) an outer layer composed of a stack of calcite lamellae.

Radiolitid shells typically disintegrated by spalling of the upper valve into its ostracal (calcitic) portion and the hypostracal (aragonitic) portion. The ostracum of the upper valve split into layer a and b, and into stacks of calcite lamellae and individual calcite lamellae of layer b. The lower valve disintegrated by spalling along radial funnel plates, and by disintegration and selective removal of the boxwork ostracum. The specific style of disintegration was aided or induced by discontinuities in the structure of the shell. The lamellar fragments from the calcitic portion of the upper valve and from the radial funnel plates of the lower valve locally are abundant in free-valve – funnel-plate floatstones. These floatstones were exclusively observed in association with radiolitid biostromes, and comprise the matrix of or occur in lenses intercalated within the biostromes.

In biostromes with an open, parautochthonous fabric the selective removal of the boxwork ostracum of the lower valve occurred by spalling and, most probably, by early diagenetic dissolution. Where the selective removal of the boxwork was complete, a thin, relict shell composed of the inner 'ostracal layer 3' and the hypostracum remained. In radiolitid biostromes with an open, parautochthonous fabric, some or all of the lower valves may show more-or-less advanced stages of selective boxwork dismantling.

During early diagenesis, the hypostracum of the shells was either replaced by blocky calcite spar or was dissolved and became filled by internal sediments. Locally, the selective removal of the boxwork ostracum and early diagenetic dissolution of aragonite combined to result in ghost biostromes. These biostromes entirely or largely consist of radiolitid relics each composed of the crescent-shaped sedimentary fills of the intertabular spaces, hosted by the thin 'ostracal shell layer 3'.

The formation of radiolitid relics by selective removal of the boxwork ostracum, and the presence of ghost biostromes produced by biostratinomic and early diagenetic processes, indicates that rudist biostromes can undergo marked taphonomic loss during fossilization. The trophic structure of a future ghost biostrome was characterized by both epifaunal suspension feeders and infaunal burrowing organisms. The presence of relict radiolitid shells in ghost biostromes with a burrowed, open parautochthonous rudist fabric indicates that the final preservation of a rudist biostrome was directly influenced by the characteristics of the entire living community, including the unpreserved burrowing taxa. Rudist biostromes thus may be of markedly different trophic structure and taphonomy as a result of the total population composition (preserved and unpreserved) and the density of substrate colonization by rudists.

Acknowledgements. Josep Maria Pons, Barcelona, and Iwan Stössel, Zürich, provided valuable discussions on the sedimentology of rudist biostromes during field trips in Austria, Italy and Spain. Robert Stanton, College Station, is thanked for a thorough review of the paper. Monika Tessadri-Wackerle arranged the figures for final layout. Financial support from project 10719-GEO from the Austrian Research Foundation is gratefully acknowledged.

References

Alsharhan, A.S. 1995: Facies variation, diagenesis, and exploration potential of the Cretaceous rudist-bearing carbonates of the Arabian Gulf. *American Association of Petroleum Geologists Bulletin 79*, 531–550.

Amico, S. 1978: Recherches sur la structure du test des Radiolitidae. *Travaux du Laboratoire de Géologie historique et de Paléontologie 8*, 1–131. Université de Provence, Marseille.

Bebout, D.G. & Loucks, R.G. (eds.) 1977: Cretaceous carbonates of Texas and Mexico. Applications to Subsurface Exploration. *Bureau of Economic Geology and University of Texas at Austin, Report of Investigations 89*. 332 pp.

Cestari, R. & Sartorio, D. 1995: *Rudists and Facies of the Periadriatic Domain*. 207 pp. Agip, San Donato Milanese.

Coe, W.R. 1957: Fluctuations in littoral populations. *In* Hedgpeth, J. (ed.): Treatise on marine ecology and paleoecology, 935–940. *Geological Society of America Memoir 67*.

Enos, P. 1988: Evolution of pore space in the Poza Rica trend (Mid-Cretaceous, Mexico). *Sedimentology 35*, 287–325.

Fürsich, F.T. & Aberhan, M. 1990: Significance of time-averaging for paleocommunity analysis. *Lethaia 23*, 143–152.

Kennedy, W.J. & Taylor, J.D. 1968: Aragonite in rudists. *Proceedings of the Geological Society of London 1645*, 325–331.

Koch, R., Ogorelec, B. & Orehek, S. 1989: Microfacies and diagenesis of Lower and Middle Cretaceous carbonate rocks of NW-Yugoslavia (Slovenia, Trnovo Area). *Facies 21*, 135–170.

Kühn, O. 1967: Rudistenhorizonte als ökologische und stratigraphische Indikatoren. *Geologische Rundschau 56*, 186–189.

Lawrence, D.R. 1968: Taphonomy and information losses in fossil communities. *Geological Society of America Bulletin 79*, 1315–1330.

Minero, C.J. 1988. Sedimentation and diagenesis along an island-sheltered platform margin, El Abra Formation, Cretaceous of Mexiko. *In* James, N.P. & Choquette, P.W. (eds.): *Paleokarst*, 385–406. Springer, New York, N.Y.

Pons, J.M. 1977: Estudio estratigrafico y paleontologico de los yacimientos de rudistidos del Cretacico Superior del Prepireneo del la Provincia de Lerida. *Universitat Autónoma de Barcelona, Publicaciones de Geologia 3*. 105 pp.

Pons, J.M. 1982: Distribucion de los rudistas (Bivalvia) del Cretacico Superior sudpirenaico. *Cuadernos de Geologia Ibérica 8*, 1027–1033.

Pons, J.M. & Vicens, E. 1986: Nuevos datos sobre *Biradiolites chaperi* (Bivalvia: Radiolitidae) del Maastrichtiense. *Revista d'investigacions geologiques 42–43*, 67–75.

Revelle, R. & Emery, K.O. 1957: Chemical erosion of beach rock and exposed reef rock. *United States Geological Survey Professional Paper 260-T*, 699–709.

Ross, D.J. & Skelton, P.W. 1993: Rudist formations of the Cretaceous: a paleoecological, sedimentological and stratigraphical review. *In* Wright, P. (ed.): *Sedimentology Review 1*, 73–91. Blackwell, Oxford.

Sanders, D. 1996a: Rudist biostromes on the margin of an isolated carbonate platform: The Upper Cretaceous of Montagna della Maiella, Italy. *Eclogae geologicae Helvetiae 89*, 845–871.

Sanders, D. 1996b: A classification of elevator rudist biostromes (Abstract). *In: Fifth International Cretaceous Symposium and Second Workshop on Inoceramids. Freiberg University of Mining and Technology*, 153.

Sanders, D. 1998a: Upper Cretaceous rudist formations. Proceedings from the Fourth Meeting of the Austrian Paleontological Society. *Geologisch-Paläontologische Mitteilungen Innsbruck 23*, 37–59.

Sanders, D. 1998b: Tectonically controlled Late Cretaceous terrestrial to neritic deposition, Gosau Group, Northern Calcareous Alps (Tyrol, Austria). *Facies 39*, 139–178.

Sanders, D. & Baron-Szabo, R.C. 1997: Coral–rudist bioconstructions in the Upper Cretaceous Haidach section (Northern Calcareous Alps, Austria). *Facies 36*, 69–90.

Sanders, D., Kollmann, H. & Wagreich, M. 1997: Sequence development and biotic assemblages on an active continental margin: The Turonian–Campanian of the Northern Calcareous Alps. *Bulletin de la Société géologique de France 168*, 351–372.

Sanders, D. & Pons, J.M. 1999: Rudist formations in mixed siliciclastic–carbonate depositional environments, Upper Cretaceous, Austria: Stratigraphy, sedimentology, and models of development. *Palaeogeography, Palaeoclimatology, Palaeoecology 148*, 249–284.

Scott, R.W. 1978: Approaches to trophic analysis of paleocommunities. *Lethaia 11*, 1–14.

Skelton, P.W. 1976: Functional morphology of the Hippuritidae. *Lethaia 9*, 83–100.

Skelton, P.W. 1978: The evolution of functional design in rudists (Hippuritacea) and its taxonomic implications. *Philosophical Transactions of the Royal Society of London B 284*, 305–318.

Skelton, P.W., Gili, E., Vicens, E. & Obrador, A. 1995: The growth fabric of gregarious rudist elevators (hippuritids) in a Santonian carbonate platform in the southern Central Pyrenees. *Palaeogeography, Palaeoclimatology, Palaeoecology 119*, 107–126.

Staff, G.M., Stanton, R.J., Jr., Powell, E.N. & Cummins, H. 1986: Time-averaging, taphonomy, and their impact on paleocommunity reconstruction: Death assemblages in Texas bays. *Geological Society of America Bulletin 97*, 428–443.

Stanton, R.J. & Dodd, J.R. 1976: The application of trophic structure of fossil communities in paleoenvironmental reconstruction. *Lethaia 9*, 327–342.

Toucas, A. 1903: Classification et l'évolution des hippuritidés. *Mémoires de la Société géologique de France 30*. 127 pp.

Toucas, A. 1907: Classification et l'évolution des radiolitidés. *Mémoires de la Société géologique de France 36*. 129 pp.

Walter, L.M. & Burton, E.A. 1990: Dissolution of recent platform carbonate sediments in marine pore fluids. *American Journal of Science 290*, 601–643.

Zapfe, H. 1937: Paläobiologische Untersuchungen an Hippuritenvorkommen der nordalpinen Gosauschichten. *Verhandlungen der Zoologisch–Botanischen Gesellschaft in Wien 86/87*, 73–124.